Available online at www.sciencedirect.com

ScienceDirect

IFAC PapersOnLine 51-30 (2018) 95–100

UD Factorization Based Non-Traditional Attitude Estimation of Nanosatellite with Rate Gyros FDI

Demet Cilden-Guler*, Chingiz Hajiyev **

** Faculty of Aeronautics and Astronautics, Istanbul Technical University, 34469, Istanbul, Turkey and Faculty of Engineering and Natural Sciences, Istanbul Medeniyet University, 34700, Istanbul, Turkey (e-mail: cilden@itu.edu.tr).*
*** Faculty of Aeronautics and Astronautics, Istanbul Technical University, 34469, Istanbul, Turkey (e-mail: cingiz@itu.edu.tr)}*

Abstract: An attitude and rate estimation method with nontraditional approach is presented for the nanosatellite having magnetometer, sun sensor and rate gyros. The approach is based on the singular value decomposition (SVD) aided extended Kalman filter (EKF). Here, EKF uses the measurements after the SVD stage as it provides linear measurements of the attitude angles and their error covariance. In this stage, measurement error covariance matrix is factorized and the measurements are reformed using UD decomposition. In the filtering stage, a fault detection and isolation method for nanosatellite rate gyros is presented based on using the corresponding innovation sequence. The innovations are used to find where and when the gyroscope faults occurred and determine the corresponding scale factor values of the rate gyros of the nanosatellite. In presence of measurement sensor fault, the isolation process finds on which axis of the rate gyro failure occurred.

Keywords: nanosatellite, attitude estimation, fault detection and isolation, rate gyro.

1. INTRODUCTION

Nanosatellites at low Earth orbits use magnetometers commonly as the magnetic field strength is strong at these levels. Second, direction of the Sun has significant roles on the equipment vulnerable to the Sun, the power system etc.; therefore, sun sensors are also used for different purposes in addition to the attitude determination. Third, rate gyros are preferred in order to have information on the angular rates of the nanosatellite motion. Those three sensors are considered in this paper as attitude and rate sensors of the nanosatellite. In order to determine the attitude, reference directions should be defined and utilized with the sensor outputs. The vector pairs can be placed in a single-frame method which is to minimize the Wahba's loss function (Wahba, 1965) for obtaining the attitude angles as measurements and their measurement error covariance. These can be processed under Kalman filtering algorithm to estimate the attitude angles and rates of the nanosatellite.

Extended Kalman filter (EKF) can be applied for estimation the attitude by assigning initial values, integrating the measurements under the propagation model of the nanosatellite dynamics. The traditional approach uses the nonlinear measurements of reference directions (DaForno et al., 2004; Sekhavat et al., 2007) while non-traditional approach linear measurements (Hajiyev & Bahar, 2003; Hajiyev et al., 2016). Review on those two approaches is carried out by (Hajiyev & Cilden Guler, 2017). The non-traditional approach based on the linear measurements is used in several studies (Hajiyev & Bahar, 2003; Hajiyev et al., 2016).

In this paper, singular value decomposition (SVD) is used as the single-frame method in the first stage because of its robustness performance (Cilden Guler et al., 2017; Markley & Mortari, 2000). The studies on non-traditional approaches consider the non-diagonal elements of the covariance matrix of the SVD to be small compared to the diagonal elements; therefore, remove those. However, in this study, an SVD-aided EKF method using UD factorization is considered in order not to neglect the non-diagonal elements but decomposed them with forming the measurements too (Grewal & Andrews, 2001). In the filtering stage, the reshaped attitude angles from SVD method after UD factorization are used as measurement inputs. For the angular velocity, rate gyro measurements are considered in the filter. For the rate gyro failure, fault detection and isolation (FDI) is applied in order to find where and when the fault is occurred.

The structure of this paper is as follows. In Section 2, the measurement models are given. In Section 3, the single-frame method, SVD is introduced. In Section 4, the non-traditional filter, SVD aided EKF is presented with the UD decomposition implementation. In Section 5, rate gyro FDI method is defined. The analysis of the simulations is presented in Section 6 and the conclusions are given in Section 7.

2. MEASUREMENT MODELS

Two attitude sensors are considered in this study to estimate the attitude using SVD-aided EKF. Magnetometer and sun sensor measurements should be modelled in order to obtain the first-step-measurements by SVD.

IGRF model defines the magnetic field direction vector (Thébault et al., 2015) in orbit frame. Here, the magnetometer measurements are needed to be modelled too. Three on-board magnetometers of the satellite measure the components of the magnetic field vector in the body frame. Therefore, for the

Peer review under responsibility of International Federation of Automatic Control.
10.1016/j.ifacol.2018.11.255

measurement model, which characterises the measurements in the body frame, gained magnetic field terms must be transformed by the use of direction cosine matrix, A. Overall measurement model may be given as;

$$B_m(k) = A(k)\,B_o(k) + v_B(k)\,, \tag{1}$$

where $B_m(k)$ is the measured Earth magnetic field vector as the direction cosines in the body frame, $v_B(k)$ is the magnetometer measurement noise. The Sun direction vector measurements can be expressed in the following form:

$$S_m(k) = A(k)S_o(k) + v_S(k)\,, \tag{2}$$

where $S_m(k)$ is the measured Sun direction vector as the direction cosines in the body frame, $S_0(k)$ represent the Sun direction vector in the orbit frame as a function of time and orbit parameters, $v_S(k)$ is the sun sensor measurement noise. The rate gyro measurements can be modelled as,

$$\omega_{BI_m}(k) = \omega_{BI}(k) + v_g(k) \tag{3}$$

where $\omega_{BI} = \begin{bmatrix}\omega_x & \omega_y & \omega_z\end{bmatrix}^T$ is the angular velocity vector of the body frame with respect to the inertial frame, $v_g(k)$ is the rate gyro measurement noise.

3. SINGLE-FRAME METHOD: SINGULAR VALUE DECOMPOSITION (SVD)

In this section, the Singular Value Decomposition (SVD) method which is one of the single-frame methods is briefly described. The basic idea of the single-frame methods is to minimize the loss defined by (Wahba, 1965).

$$L(A) = \frac{1}{2}\sum_i a_i \,|\, \mathrm{b}_i - \mathrm{Ar}_i \,|^2 \tag{4}$$

$$B = \sum a_i b_i r_i^T \tag{5}$$

$$L(A) = \lambda_0 - tr\left(AB^T\right) \tag{6}$$

where b_i is the unit vector measurements in body, r_i is the unit vector from theoretical model in reference, a_i is the non-negative weights, λ_0 is the sum of non-negative weights. Here, maximizing the trace $\left(tr(\mathrm{AB}^T)\right)$ is the same with minimizing the loss function (L). Minimization can be achieved using SVD (Markley & Mortari, 2000).

$$B = USV^T = Udiag\left|S_{11}\ S_{22}\ S_{33}\right|V^T \tag{7}$$

$$A_{opt} = Udiag[1 \quad 1 \quad \det(U)\det(V)]V^T \tag{8}$$

where U, V are orthogonal left and right matrices respectively, $\left(S_{11},\, S_{22},\, S_{33}\right)$ are the primary singular values. The coarse attitude angles can be obtained using the optimal transformation matrix A_{opt}. Moreover, rotation angle error covariance matrix $\left(P_{SVD}\right)$ can also be calculated as,

$$P_{SVD} = Udiag[(\mathrm{s}_2+\mathrm{s}_3)^{-1} \quad (\mathrm{s}_3+\mathrm{s}_1)^{-1} \quad (\mathrm{s}_1+\mathrm{s}_2)^{-1}]U^T \tag{9}$$

where secondary singular values are $s_1 = S_{11},\ s_2 = S_{22},\ s_3 = det(U)det(V)\ S_{33}$.

4. NON-TRADITIONAL ATTITUDE ESTIMATION METHOD: SVD-AIDED EKF

The non-traditional structure uses the processed attitude angle measurements which are linear and P_{SVD} of Section 3. Therefore, the measurements used in the filter include 6 elements as,

$$z(k) = \begin{bmatrix} \varphi(k) + v_\varphi(k) \\ \theta(k) + v_\theta(k) \\ \psi(k) + v_\psi(k) \\ \omega_x(k) + v_{g_x}(k) \\ \omega_y(k) + v_{g_y}(k) \\ \omega_z(k) + v_{g_z}(k) \end{bmatrix} \tag{10}$$

where the first three represent the attitude angle measurements from SVD, and the last three are the rate gyro measurements. In order to use the measurement covariance matrix from the SVD directly in the filter, a diagonalization of the P_{SVD} is done using UD decomposition right after the SVD. The factorized matrix is then called $\tilde{R}$ and used in the filter as the diagonal measurement noise covariance matrix. As it is factorized, the measurement vector from the SVD method is also redefined (Grewal & Andrews, 2001; Saha, 2003). If the measurement vector z coming from the single-frame method, SVD is defined as,

$$z = Hx + v \tag{11}$$

corresponding covariance matrix which is not diagonal matrix can be represented as,

$$E\left[vv^T\right] = P_{SVD} = R \tag{12}$$

UD can also be called modified Cholesky decomposition seen in elemental matrix form as,

$$\begin{array}{ccccccc} \mathrm{P}_{SVD} & = & U & \times & D & \times & U^T \\ \begin{bmatrix} r_{11} & r_{12} & r_{13} \\ r_{21} & r_{22} & r_{23} \\ r_{31} & r_{32} & r_{33} \end{bmatrix} & = & \begin{bmatrix} 1 & u_{12} & u_{13} \\ 0 & 1 & u_{23} \\ 0 & 0 & 1 \end{bmatrix} & & \begin{bmatrix} d_{11} & 0 & 0 \\ 0 & d_{22} & 0 \\ 0 & 0 & d_{33} \end{bmatrix} & & \begin{bmatrix} 1 & 0 & 0 \\ u_{21} & 1 & 0 \\ u_{31} & u_{32} & 1 \end{bmatrix} \end{array} \tag{13}$$

The loop can be composed using i and j variables with the row/column size of n for R matrix.

$$\begin{aligned} & n = length(R) \\ \text{Init:} \quad & U = D = zeros(n) \\ & D_{nn} = R_{nn} \\ & U_{in} = \begin{Bmatrix} i & i = n \\ R_{in} / D_{nn} & i = n-1, n-2, \ldots, 1 \end{Bmatrix} \end{aligned} \tag{14}$$

$$j \in \{n-1, n-2, \ldots, 1\}$$

$$D_{jj} = R_{jj} - \sum_{k=j+1}^{n} D_{kk} U_{jk}^2 \tag{15}$$

$$U_{ij} = \left\{ \begin{array}{cc} 0 & i > j \\ 1 & i = j \\ \left(R_{ij} - \sum_{k=j+1}^{n} D_{kk} U_{ik} U_{jk} \right) & i = j-1, \ldots, 1 \end{array} \right\}$$

Covariance matrix (R) can be factored in order to find diagonalized and uncorrelated matrix (D) consisting of the pivots in addition to the unit upper triangular part (U) whose diagonal entries are equal to 1 and forms the measurement vector again.

$$R = UDU^T \tag{16}$$

$$\tilde{z} = U^{-1} z = U^{-1}(Hx + v) = (U^{-1}H)x + (U^{-1}v) = \tilde{H}x + \tilde{v} \tag{17}$$

The "new" measurement $\tilde{z}$ has measurement matrix $\tilde{H} = U^{-1}H$ and measurement noise $\tilde{v} = U^{-1}v$. The covariance matrix $\tilde{R}$ of the measurement noise $\tilde{v}$ is determined as (Grewal & Andrews, 2001),

$$\tilde{R} = E\left[\tilde{v}\tilde{v}^T\right] = D \tag{18}$$

Newly composed $\tilde{R}$ and $\tilde{z}$ can be used in the Kalman filter in order to be updated automatically by the single-frame output. The state vector is composed of attitude angles and the angular rates with 6 elements. The Extended Kalman Filter (EKF) algorithm with the aid from SVD is given in this section.

Innovation sequence,

$$\Delta(k+1) = \{\tilde{z}(k+1) - H\hat{x}(k+1/k)\} \tag{19}$$

Equation of the estimation value,

$$\hat{x}(k+1) = \hat{x}(k+1/k) + K(k+1) \times \Delta(k+1) \tag{20}$$

Here $\tilde{z}(k+1)$ is the measurement vector, H is the measurement matrix, $\Delta(k+1)$ is the innovation sequence. In the investigated case the measurement matrix composed of a unit matrix. $H = \mathrm{diag}([1 \quad 1 \quad 1 \quad 1 \quad 1 \quad 1]) = I_{6\times6}$ measurement matrix is used. Normalized innovations can be obtained as $\left\{\hat{\Delta}(k+1) = \Delta(k+1) \times \left[HP(k+1/k)H^T + \tilde{R}(k)\right]^{-0.5}\right\}$.

Equation of the extrapolation value,

$$\hat{x}(k+1/k) = f\left[\hat{x}(k), k\right] \tag{21}$$

Filter-gain of EKF is,

$$K(k+1) = P(k+1/k)H^T(k+1) \times\left[H(k+1)P(k+1/k)H^T(k+1) + \tilde{R}(k)\right]^{-1} \tag{22}$$

The covariance matrix of the extrapolation error is,

$$P(k+1/k) = \frac{\partial f[\hat{x}(k), k]}{\partial \hat{x}(k)} P(k/k) \frac{\partial f^T[\hat{x}(k), k]}{\partial \hat{x}(k)} + Q(k) \tag{23}$$

The covariance matrix of the filtering error is,

$$P(k+1/k+1) = \left[I - K(k+1)H(k+1)\right]P(k+1/k) \tag{24}$$

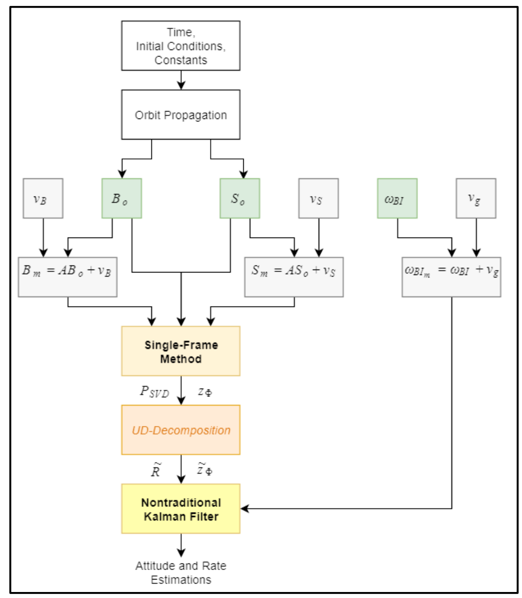

Fig. 1. Non-traditional attitude and rate estimation block diagram with UD factorization.

$\tilde{R}$ is the diagonalized covariance matrix of measurement noise and Q is the covariance matrix of the system noises. Here, (19) - (24) represent the Extended Kalman Filter (EKF), which fulfils recursive estimation of the satellite's rotational motion parameters about its mass centre on the linear attitude measurements. The whole algorithm scheme for non-traditional estimation can be seen in Fig. 1 including the sub-step of UD decomposition.

5. RATE GYRO FDI BASED ON THE MULTIPLE MEASUREMENT NOISE SCALE MATRIX

Faults on the sensors can be detected and isolated using the innovation sequence defined in (19) in the formula of multiple measurement noise scale matrix. For this purpose, the real and theoretical values of the innovation covariance matrix must be compared.

When there is a measurement malfunction in the estimation system, the real error will exceed the theoretical one. Hence, if a multiple measurement noise scale matrix, $S(k)$, is added into the algorithm as (Hajiyev, 2016)

$$\frac{1}{M} \sum_{j=k-M+1}^{k} \Delta(j)\Delta^T(j) = H(k)P(k/k-1)H^T(k) + S(k)R(k) \tag{25}$$

then, it can be determined by the formula of,

$$S(k)=\left(\left\{\frac{1}{M}\sum_{j=k-M+1}^{k}\Delta(j)\Delta^{T}(j)\right\}-HP(k/k-1)H^{T}\right)R^{-1}(k) \tag{26}$$

where M is the width of the sliding window. For the simulations, $M=20$ is used.

The multiple measurement noise scale matrix, $S(k)$, proposed in (Hajiyev, 2016), can be used for the gyros fault detection and isolation (FDI) purpose. In this case, the following diagonal elements of this matrix S_{ii} ($i=4,5,6$) will indicate the current state of the gyros and can be used as the monitoring statistics.

In case of normal operation of gyros, the diagonal elements S_{44}, S_{55}, S_{66} of the scale matrix will be units. Nevertheless, as M is a limited number because of the number of the measurements and the computations performed with computer implies errors such as approximation errors and round off errors; these elements may not be unit and may be negative or less than one which is physically not possible. In order to avoid such situation, composing the scale matrix by the following rule is used (Hajiyev & Soken, 2012):

$$S_{ii}^{*}=\max\{1,S_{ii}\} \qquad i=4,5,6\,. \tag{27}$$

If the condition $S_{ii}^{*}>th$ ($i=4,5,6$) is true, then the ith gyro is accepted to be faulty. Here th is the threshold value, which is determined empirically through experience.

6. SIMULATIONS

Simulations are performed for a nanosatellite orbiting around Earth at low altitudes. The principal moment of inertia matrix is $J=diag\left(2.1\times10^{-3}\quad 2.0\times10^{-3}\quad 1.9\times10^{-3}\right)$. For the magnetometer measurements, the sensor noise is characterized by zero mean Gaussian white noise with a standard deviation of $\sigma_m=300\ nT$. The standard deviation for the sun sensor noise is taken as $\sigma_s=0.002$ (for unit vector measurements).

Since the computational sources are not sufficient at small satellites, it is better to use the measurement covariance matrix as diagonal to reduce the computational burden. There are two ways in order to use this matrix diagonal. First is to neglect the non-diagonal terms with Assumption and the second is to use the UD factorization. For analysing the simulation results, both methods are considered and compared. For both, SVD-aided EKF algorithm works recursively.

6.1. Gyros without any failure

In order to simulate the three-axis rate gyros, (3) is used. The estimation of the pitch angle can be seen in Fig. 2 in the first panel, errors in the second and the related variance in the third. Other attitude angles roll and yaw are having the similar results. As it can be seen from the figure that the SVD-aided EKF improve the attitude estimations as expected.

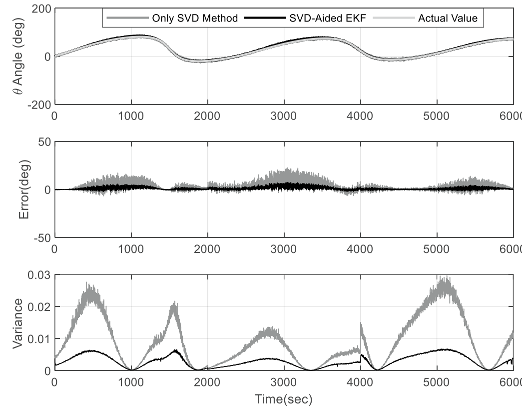

Fig. 2. Pitch angle estimations, error and variance of only SVD and SVD-aided EKF using UD factorization.

Table 1. RMSE results of attitude angles with and without UD factorization.

RMSE (deg)	Roll	Pitch	Yaw
With UD	0.0495	0.0782	0.0669
With Assumption	0.0350	0.0538	0.0614

Table 1 gives the RMSE of each attitude angle estimation with UD and with assumption. The simulations having UD factorization for the measurement noise covariance diagonalization and measurement update is called “With UD” while the simulations assuming the measurements are uncorrelated and eliminating the non-diagonal elements of the measurement noise covariance, is called “With Assumption”. SVD-aided EKF with assumption gives the overstated accuracy of the attitude angles. In order to obtain more realistic results, UD decomposition is applied in the next section.

6.2. Gyros experiencing failure

In this section, two types of rate gyro failures are applied in this study not on the other attitude sensors because for the sun sensor and magnetometers used on the satellites as attitude sensors, calibration is done before those measurements processed in SVD method (Ivanov et al., 2012).

6.2.1. Bias Type of Fault on the Rate Gyros

In order to simulate the gyroscopes experiencing a malfunction, first, we applied a continuous bias type of fault on the y-axis as

$$\omega_{BI_{m_y}}(k)=\omega_{BI_y}(k)+v_{g_y}(k)+b_y(k)\;,\;\left(k\geq 4000\ \text{s}\right) \tag{28}$$

Here, the bias on the y-axis is applied as $b_y=0.3$ rad/s. After the fault occurrence, a change especially on the pitch angle can be seen from the figure. The absolute error on the y axis angular rate estimations is seen in Fig. 3 as the fault is applied on the y-axis. Here, the bias effects after the 4000 seconds is pointed using a red box.

The effects of the malfunction on y-axis can be seen on the second panel of the normalized innovations ($\hat{\Delta}$) presented in Fig. 4 as it exceeds the $\pm 3\sigma$ bounds while there is a fault. Finally, MMNSF changes in time can be seen in Fig. 5. As seen, the scale factor corresponding to the y-axis rate gyro exceeds the threshold value, three, while the rest of them lay between the allowable limits.

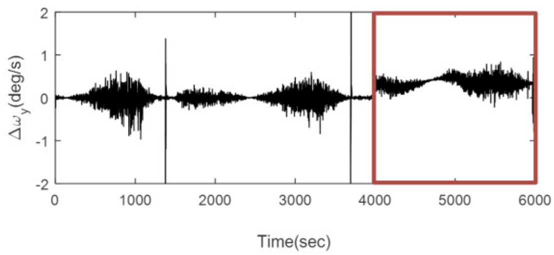

Fig. 3. Angular rate estimation error on y-axis.

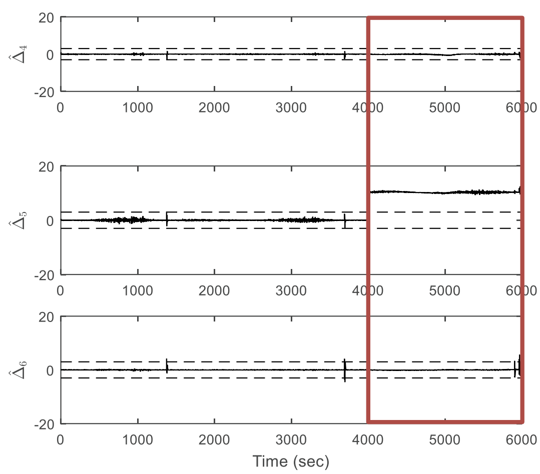

Fig. 4. Normalized innovation change in time for each axis of the angular rate part.

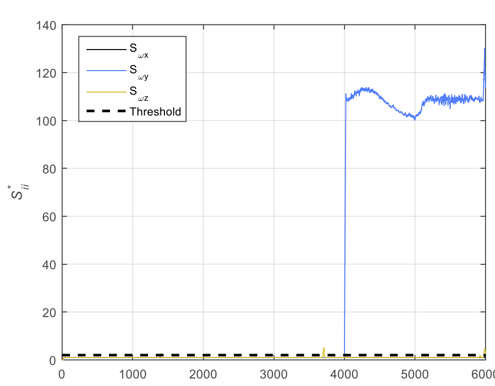

Fig. 5. Multiple measurement noise scale factor changes in time for each axis of the angular rate part.

We presented the simulation results for the continuous bias type of fault on y-axis gyro measurements after 4000 seconds. The diagonal elements $S^*_{44}, S^*_{55}, S^*_{66}$ of the multiple measurement noise scale matrix, $S^*(k)$ at the 4050[th] second of simulation (50 s after the rate gyro failure occurs) are $\left(S^*_{44}=1\right)$, $\left(S^*_{55}=25\right)$, $\left(S^*_{66}=1\right)$. The third diagonal element S^*_{55} of the scale matrix, which correspond to the y-axis rate gyro scale factor is significantly larger and exceeds the threshold value. Consequently, the y-axis rate gyro failure is detected and isolated.

6.2.2. Noise Increment Type of Fault on the Rate Gyros

For the second scenario, noise increment type of fault is utilized on the y-axis of the rate gyros as.

$$\omega_{BI_{m_y}}(k) = \omega_{BI_y}(k) + 40 \times v_{g_y}(k)\,,\quad \left(k \geq 4000\text{ s}\right) \tag{29}$$

The absolute error on the y axis angular rate estimations is seen in Fig. 6 as the fault is applied on the y-axis. Here, the noise increment effects after the 4000 seconds is pointed using a red box.

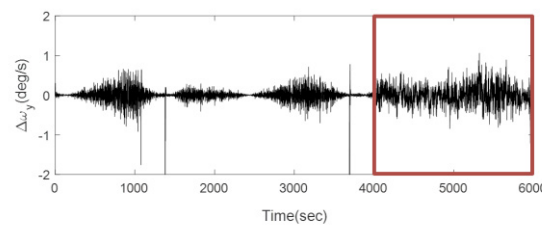

Fig. 6. Angular rate estimation error on y-axis.

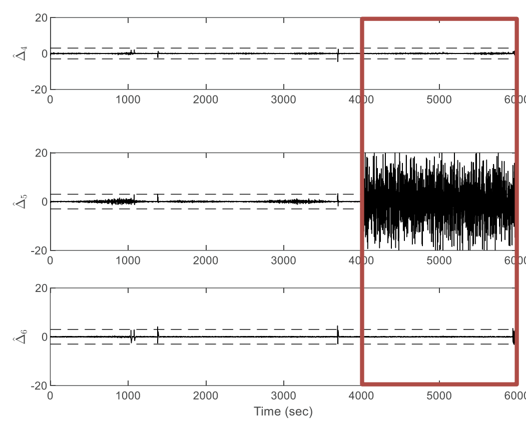

Fig. 7. Normalized innovation change in time for each axis of the angular rate part.

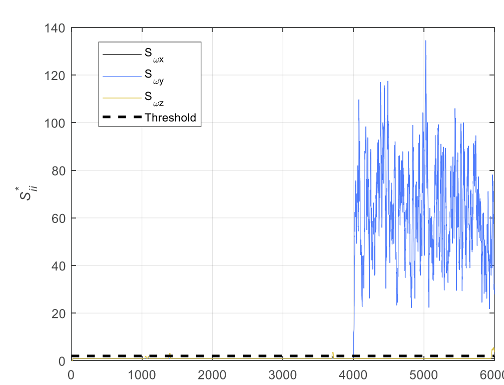

Fig. 8. Multiple measurement noise scale factor changes in time for each axis of the angular rate part.

The effects of the malfunction on y-axis can be seen on the second panel of the normalized innovations ($\hat{\Delta}$) presented in Fig. 7 as it exceeds the $\pm 3\sigma$ bounds while there is a fault. Finally, MMNSF changes in time can be seen in Fig. 8. As seen, the scale factor corresponding to the y-axis rate gyro exceeds the threshold value, three, while the rest of them lay between the allowable limits.

In this section, the noise increment is applied on y-axis gyro measurements after 4000 seconds. The corresponding diagonal elements at the 4050[th] second (50 s after the rate gyro failure) are $\left(S_{44}^{*}=1\right)$, $\left(S_{55}^{*}=18.5\right)$, $\left(S_{66}^{*}=1\right)$. Here, the fifth diagonal element S_{55}^{*} of the scale matrix, is significantly larger which means that the y-axis rate gyro failure is detected and isolated.

7. CONCLUSIONS

In this paper, non-traditional attitude and rate estimation approach, SVD-aided EKF having the inputs from SVD as the linear measurements of attitude angles and their error covariance is presented. For diagonalization of the measurement noise covariance matrix, UD is used as it is factorizing the attitude angles error covariance with forming the measurements in order to obtain the appropriate inputs for the EKF. For the integrated SVD/EKF using the newly formed measurements and measurement noise covariance with UD factorization, the whole algorithm is run. Simulation results show that the SVD-aided EKF with assumption which acts that the measurements are uncorrelated and removes the non-diagonal elements of the measurement noise covariance gives the understated accuracy of the attitude angles. However, the proposed attitude estimation method with UD factorization provides the exact value of attitude accuracy.

For the satellites having gyros might experience a failure on their sensors. In order to detect and isolate the fault, rate gyro FDI based on innovation sequence is presented. By using this method, it can be determined on which axis the rate gyro failure is. In presence of measurement faults, the isolation process performs well by using the proper threshold.

ACKNOWLEDGEMENTS

The author D. Cilden-Guler is supported by ASELSAN (Military Electronic Industries) and TUBITAK (Scientific and Technological Research Council of Turkey) PhD Scholarships.

REFERENCES

Cilden Guler, D., Conguroglu, E. S., and Hajiyev, C. (2017). Single-Frame Attitude Determination Methods for Nanosatellites. *Metrology and Measurement Systems*, *24* (2), 313–324. https://doi.org/10.1515/mms-2017-0023

DaForno, R., Reali, F., Bristor, S., and Debei, S. (2004). Autonomous Navigation of MegSat1: Attitude, Sensor Bias and Scale Factor Estimation by EKF and Magnetometer-Only Measurement. In *22nd AIAA International Communications Satellite Systems Conference and Exhibit*. California, USA. https://doi.org/10.2514/6.2004-3183

Grewal, M. S., and Andrews, A. P. (2001). *Kalman Filtering: Theory and Practice Using MATLAB*.

Hajiyev, C. (2016). An Innovation Approach Based Sensor Fault Detection and Isolation. *IFAC-PapersOnLine*, *49* (17), 420–425. https://doi.org/10.1016/J.IFACOL.2016.09.072

Hajiyev, C., and Bahar, M. (2003). Attitude Determination and Control System Design of the ITU-UUBF LEO1 Satellite. *Acta Astronautica*, *52* (2–6), 493–499.

Hajiyev, C., Cilden, D., and Somov, Y. (2016). Gyro-Free Attitude and Rate Estimation for a Small Satellite using SVD and EKF. *Aerospace Science and Technology*, *55* , 324–331. https://doi.org/http://dx.doi.org/10.1016/j.ast.2016.06.004

Hajiyev, C., and Cilden Guler, D. (2017). Review on Gyroless Attitude Determination Methods for Small Satellites. *Progress in Aerospace Sciences*, *90* , 54–66. https://doi.org/10.1016/j.paerosci.2017.03.003

Hajiyev, C., and Soken, H. E. (2012). Robust Estimation of UAV Dynamics in the Presence of Measurement Faults. *Journal of Aerospace Engineering*, *25* (1), 80–89. https://doi.org/10.1061/(ASCE)AS.1943-5525.0000095

Ivanov, D. S., Roldugin, D. S., Tkachev, S. S., Tkachev, S. S., Karpenko, S. O., Ivlev, N. A., and Ovchinnikov, M. Y. (2012). Chibis-M Microsatellite Attitude Control Algorithms Work Analysis (in Russian). In G. A. Avanesov (Ed.), *TheThird All-Russian Scientific and Technological Conference: "Contemporary Problems of Spacecraft Attitude Determination and Control"* pp. 114–131. Tarusa, Russia.

Markley, F. L., and Mortari, D. (2000). Quaternion Attitude Estimation using Vector Observations. *Journal of Astronautical Sciences*, *48* , 359–380.

Saha, S. K. (2003). Simulation of Industrial Manipulators Based on the UDU T Decomposition of Inertia Matrix. *Multibody System Dynamics*, *9* (1), 63–85. https://doi.org/10.1023/a:1021659722559

Sekhavat, P., Gong, Q., and Ross, I. M. (2007). NPSAT I Parameter Estimation using Unscented Kalman Filter. In *Proc. 2007 American Control Conference* pp. 4445–4451. New York, USA. https://doi.org/10.1109/ACC.2007.4283031

Thébault, E., Finlay, C. C., Beggan, C. D., Alken, P., and Al., E. (2015). International Geomagnetic Reference Field: the 12th generation. *Earth, Planets and Space*, *67* (1), 79. https://doi.org/10.1186/s40623-015-0228-9

Wahba, G. (1965). Problem 65-1: A Least Squares Estimate of Satellite Attitude. *Society for Industrial and Applied Mathematics Review*, *7* (3), 409. Retrieved from http://www.malcolmdshuster.com/FC_Wahba_1965_J_SIAM.pdf